Applied Research

Applied Research

RESEARCH ARTICLE OPEN ACCESS

Starch Phosphate Carbamate Synthesis in the Age of Machine Learning: Maximization of the Phosphorus Content and the Educt Efficiency via Bayesian Optimization

Florian Rothenhäusler[1] | Simon Knorr[2] | Seema Agarwal[2] | Holger Ruckdaeschel[1]

[1]Department of Polymer Engineering, University of Bayreuth, Bayreuth, Germany | [2]Macromolecular Chemistry II, University of Bayreuth, Bayreuth, Germany

Correspondence: Holger Ruckdaeschel (holger.ruckdaeschel@uni-bayreuth.de)

Received: 6 May 2025 | **Revised:** 5 December 2025 | **Accepted:** 16 February 2026

Funding: the German Federal Ministry for Economic Affairs and Climate Action (BMWK) within the research project "NewPreg – Nachhaltige, wirtschaftliche und funktionalisierte Bio-Feststoffharz-Prepregtechnologie zur CO2-Reduktion durch kühlfreie Lagerung, Einsatz erneuerbarer Ressourcen und Gewichtsreduktion durch maßgeschneidertes Drapierverhalten"

Keywords: Bayesian optimization | bio-based | flame retardant | machine learning | starch phosphate carbamates | sustainability

ABSTRACT

Starch phosphate carbamates (SPC) have been a focal point in the research and development of sustainable flame retardants (FRs) for the past two decades. Within this framework, there is a notable emphasis on obtaining SPC with a high phosphorus content. Aligning with the contemporary trend of artificial intelligence and machine learning, the optimization of synthesis conditions for specific product properties can be efficiently achieved through their utilization. Hence, the objective of this study is to optimize the synthesis conditions, including the molar ratio of anhydroglucose units to urea and phosphoric acid, as well as the synthesis temperature and duration. The optimization is conducted via Bayesian optimization, aiming to maximize the phosphorus content and educt efficiency of SPC to obtain a potent, bio-based FR. As a result, the phosphorus content and educt efficiency are increased to about 20.5% and 11.3%/mol, respectively.

1 | Introduction

Starch phosphate carbamates (SPC) have garnered significant attention in the realm of sustainable flame retardants (FRs) over the past two decades [1–12]. These compounds have found application as FRs across a diverse array of matrix materials, including wood, polystyrene foams, paper, cotton, and thermosets [13–17]. SPC represent a combination of starch, a cost-effective and natural feedstock, with the flame-retardant attributes of phosphates [18–20]. The phosphatization process of SPC occurs in the presence of urea and a phosphatizing agent within the temperature range of 120°C–150°C for several hours. The hydroxyl groups of the anhydroglucose units (AGU) undergo transformation into various esters, encompassing functional groups like phosphate, ammonium phosphates, and carbamate groups (refer to Figure 1) [1, 7]. The molar ratio between the AGU of starch, urea, and the phosphatizing agent plays a pivotal role in achieving a high phosphorus content in SPC, predominantly in the form of ammonium phosphate type functional groups [10]. Heinze and colleagues underscored that a molar ratio between urea and the phosphatizing agent of at least three is crucial for the successful synthesis of SPC with a high phosphorus content [1].

In chemistry, the synthesis conditions for SPC, including the molar ratios of reagents, synthesis temperature, and duration,

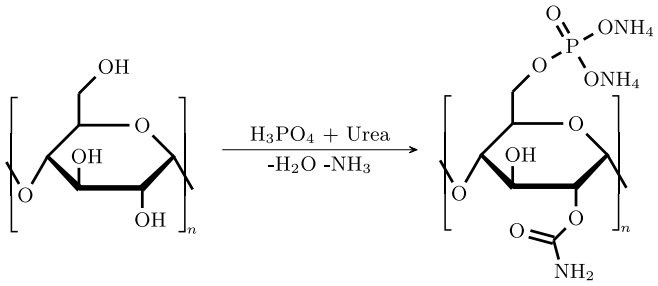

FIGURE 1 | Synthesis of SPC using phosphoric acid and urea.

have traditionally been derived empirically, often through trial-and-error approaches on a limited subset of potential permutations of conditions [1]. Comparing results from synthesis conditions that vary only in one parameter, such as synthesis duration, has provided insights into trends within the data set but falls short of predicting an optimized set of conditions for specific SPC properties. Given the heightened interest in SPC as bio-based FR, maximizing their phosphorus content emerges as a logical objective. Recent advances in the integration of machine learning and chemical synthesis have demonstrated the potential of such approaches to accelerate reaction optimization, reduce experimental workload, and identify nonobvious optimal conditions in complex parameter spaces [21–23]. Phosphorus-based FR mechanisms operate in both gas and condensed phases, involving processes like flame zone dilution, radical scavenging, dehydration reactions, esterification, cross-linking, and aromatization of the matrix material [24–27]. In general, a higher phosphorus content correlates with increased FR efficacy. Therefore, leveraging machine learning presents a promising avenue for optimizing distinct SPC characteristics with a constrained number of synthesis conditions, that is, phosphorus content. Bayesian optimization (BO) enables the identification of optimal synthesis conditions from a vast pool of potential experiments [28–30]. Therefore, BO offers a viable approach to optimize the molar ratios of AGU, urea, and phosphatizing agents, along with synthesis temperature and duration.

However, optimizing the synthesis conditions for only maximizing the phosphorus content of SPC might lead to a poor educt efficiency, meaning that increased molar ratios of urea and phosphoric acid to an under-proportional increase in phosphorus content. Therefore, two additional target properties are defined:

1. Phosphoric acid efficiency (P-efficiency)
2. Urea-phosphoric acid efficiency (UP-efficiency)

The P-efficiency (η_P) is defined as follows:

$$\eta_P = \frac{P_\%}{n_{PA}} \tag{1}$$

where $P_\%$ is the phosphorus content of the respective experiment and n_{PA} the molar ratio of phosphoric acid. Equivalently, the UP-efficiency (η_{UP}) is defined as:

$$\eta_{UP} = \frac{P_\%}{n_{urea} + n_{PA}} \tag{2}$$

where $P_\%$ is the phosphorus content of the respective experiment, and n_{urea} and n_{PA} are the molar ratios of urea and phosphoric acid, respectively.

In this work, each of the three target properties—$P_\%$, η_P, and η_{UP}—was optimized in independent BO runs. This approach allows the identification of synthesis conditions, meaning molar ratios of the reagents, as well as the synthesis temperature and duration, tailored specifically to each target property rather than forcing a compromise solution via multiobjective optimization. While simultaneous multiobjective optimization could, in principle, identify trade-offs between the targets, the focus here was to first determine the individual optima for each property with minimal experimental effort.

2 | Experimental

2.1 | Bayesian Optimization

2.1.1 | *Virtual Experiments*

To maximize the $P_\%$, η_P, and η_{UP} of SPC, optimization focuses on adjusting the molar ratios of urea and phosphoric acid (PA), along with the synthesis temperature and synthesis duration. A grid approach is adopted to design the virtual experiments, encompassing a broad spectrum of synthesis conditions. The molar ratio of urea ranges from 1 to 15 in increments of 0.25, while PA's ratio varies from 1 to 5 in steps of 0.25. Similarly, synthesis temperatures span between 120°C and 140°C with 5° increments, and synthesis durations range from 1 to 3 h with half-hour steps. These ranges ensure successful starch phosphatization at the lower end and offer a broader exploration of molar ratios than previous studies [1]. Each step size is carefully chosen to yield definitive results while enabling noticeable differences in phosphorus content across different sets of synthesis conditions. These parameters yield a total of 24,225 individual experiments within the virtual experiment pool.

2.1.2 | *Procedure*

For the BO process, 5 random experiments are selected from the pool of 24,225 virtual experiments as starting points. The target properties of these random starting experiments are then modeled separately using Gaussian process regression (GPR), employing a dot-product (DP) kernel and a radial basis function (RBF) kernel. This GPR model is implemented using the BayesianOptimizer module from ModAL [31, 32]. The selection of the RBF kernel function is deliberate, as it is anticipated that the optimal synthesis conditions for maximizing the target properties may not necessarily reside at the extremes of the feature space [33]. The $P_\%$ of the BO of η_P, and η_{UP} are also included in the data set for the optimization of $P_\%$ and vice versa.

In the initial optimization iteration, a range of acquisition functions is utilized to forecast promising experiments within the virtual experiment pool that are expected to yield high target properties. The outcomes of these selected experiments are subsequently incorporated into the data set for the subsequent optimization iteration. This iterative process continues until the target values, that is, the phosphorus content, the P-efficiency, and the UP-efficiency, cease to increase further.

For clarity, the optimization of $P_\%$, η_P, and η_{UP} was carried out separately. Three independent BO processes were run, each using the same pool of virtual experiments and the same initialization strategy, but with the target property defined according to the specific objective. The results of each BO run

were then compared to assess the potential trade-offs between the different optimal conditions.

2.1.3 | *Kernel Functions*

In this study, two kernel functions—RBF and DP—were employed in parallel to exploit their complementary properties in modeling the response surface of the SPC synthesis space.

The RBF kernel is well-suited for capturing smooth, localized variations in the target property space, making it advantageous when optimal conditions may lie within a restricted region rather than at the feature space boundaries [28, 31, 34]. Although its predictions tend to remain close to the initial sampling area, this characteristic enables a thorough exploration of promising local optima and avoids premature convergence to extreme, potentially unfeasible parameter settings. The RBF kernel had a length scale of 1.0 and length scale boundaries ranging from 10^{-12} to 10^{15}.

The DP kernel, in contrast, allows for modeling broader, more global trends across the search space, which facilitates the identification of promising regions even far from the initial experiments [35]. Using both kernels in combination leverages the exploratory capacity of the DP kernel while maintaining the fine-grained, local refinement capability of the RBF kernel [30]. The DP kernel had a sigma value of 1.0 and sigma boundaries ranging from 10^{-1} to 10^{3}.

Random initialization was applied to ensure broad initial coverage of the parameter space and to reduce bias toward specific synthesis regions [36]. The combination of stochastic exploration and dual-kernel modeling aims to balance exploration and exploitation, increasing the likelihood of identifying both global and local optima with a limited number of experiments.

2.1.4 | *Acquisition Function*

In this study, only the upper confidence bound was utilized as an acquisition function in the optimization process. UCB is defined as:

$$\mathrm{UCB}(\mathbf{X}) = \mu(\mathbf{X}) + \beta\sigma(\mathbf{X}) \tag{3}$$

where $\mu(\mathbf{X})$ represents the predicted mean of the GPR model for the virtual experiments $\mathbf{X}$, $\sigma(\mathbf{X})$ denotes the predictive standard deviation of the GPR model, and β is a hyperparameter controlling the balance between exploitation and exploration.

In this study, the hyperparameter β in the UCB acquisition function was set to 1. This choice follows common practice in BO, where moderate values of β (typically between 0.5 and 2) are used to balance exploitation (selecting conditions with high predicted performance) and exploration (selecting conditions with high predictive uncertainty) [34, 37]. We performed preliminary optimization trials on a small subset of the virtual experiment pool using different β values (0.5, 1, and 2) and observed no significant improvement in convergence speed or final target values compared to $\beta = 1$. Given its stable behavior, ease of interpretation, and frequent use in similar chemical optimization studies [28, 30], $\beta = 1$ was selected for all optimizations in this work.

2.2 | Materials

The wheat starch used in the experiment was procured from VWR Chemicals (Radnor, PA, USA). Urea (≥ 99.5%) was obtained from Carl Roth GmbH (Karlsruhe, Germany), while PA (85%) was sourced from Fisher Scientific GmbH (Schwerte, Germany). All chemicals were utilized in their as-received state.

2.3 | Synthesis

The wheat starch, urea, and PA were mixed in accordance with the molar ratios specified for each experiment. The resulting mixtures were then placed in a vacuum oven at 60 mbar and subjected to the temperature and duration prescribed by the experimental conditions. Subsequently, the purification of the SPC was carried out following the procedure outlined by Rothenhäusler et al. [10]. Following purification, the SPC samples were manually milled to obtain a fine powder suitable for characterization. Each synthesis condition was performed once due to the large number of conditions studied.

2.4 | Inductively Coupled Plasma Optical Emission Spectroscopy

The $P_{\%}$ of the SPC was determined using inductively coupled plasma optical emission spectroscopy (ICP-OES) with a Perkin Elmer Avio 200 spectrometer from PerkinElmer, Inc. (Waltham, MA, USA). For the measurement, a 10 mg sample was mixed with 5 mL of concentrated nitric acid and 2 mL of hydrogen peroxide solution. The mixture was digested at 185°C for 15 min with a heating rate of 8°C min^{-1} in a microwave oven. After cooling, the sample was diluted to 100 mL with deionized water and analyzed by ICP-OES at 213.617 nm. Calibration was performed using a commercially available phosphorus standard from Carl Roth GmbH (Karlsruhe, Germany). Each synthesis condition was analyzed in duplicate by ICP-OES to verify measurement reproducibility. The relative deviation between replicate measurements was consistently below 0.2%, and the values reported in Table 1 represent the average of the two replicates.

3 | Results and Discussion

Figure 2 illustrates the $P_{\%}$ values of 19 different synthesized SPC formulations, along with the current maximum $P_{\%}$ value, indicated by the orange line. As previously mentioned, the $P_{\%}$ of the BO of the various target properties is included in all models. Consequently, the BO of η_{P} and η_{UP} also incorporates the data from the BO of $P_{\%}$, and vice versa.

The BO of the SPC formulations for all target properties can be categorized into four phases. Initially, five random experiments are selected as starting points. The first BO iteration utilizes the GPR model based on these five data points. This GPR model is then refined by incorporating data points proposed by the first BO iteration (Experiments 6–10). The second iteration follows a similar approach, encompassing Experiments 11–14. Subsequently, five additional random data points are added to the data set to enhance diversity.

The number of data points in the first and second BO iterations differs because some data points are already proposed

TABLE 1 | Sample number, sample type, kernel function, n_{urea}, n_{PA}, synthesis temperature, synthesis duration, $P_{\%}$, η_P, and η_{UP} of the SPC.

#	Type	Kernel	$n_{urea}/-$	$n_{PA}/-$	$T/°C$	t/h	$P_{\%}/\%$	$\eta_P/\%/mol$	$\eta_{UP}/\%/mol$
1	RND	—	14.75	1	140	1	9.37	9.37	0.59
2	RND	—	10.5	4.25	130	1	2.18	0.51	0.15
3	RND	—	12.5	4.75	120	1.5	12.98	2.73	0.75
4	RND	—	9	1	130	1.5	10.45	10.45	1.05
5	RND	—	3	1.75	125	2	13.72	7.84	2.89
6	$P_{\%}$	DP	15	5	140	3	20.49	4.10	1.02
7	$P_{\%}$	RBF	3.25	1.75	125	2	11.53	6.59	2.31
8	η_P	DP	15	1	120	3	10.1	10.1	0.63
9	η_P	RBF	8.75	1	130	1.5	10.01	10.01	1.03
10	η_{UP}	RBF	4	1	125	3	11.31	11.31	2.26
11	$P_{\%}$	RBF	15	4.75	140	3	17.67	3.72	0.89
12	η_P	DP	14.75	1	140	3	10.21	10.21	0.65
13	η_P	RBF	3.75	1	125	3	10.68	10.68	2.25
14	η_{UP}	RBF	2.75	1.5	125	2	8.55	5.7	2.01
15	RND	—	6	4.5	140	1.5	17.93	3.98	1.71
16	RND	—	4.75	1.25	120	2.5	11.54	9.23	1.92
17	RND	—	6.75	3	140	1.5	15.31	5.10	1.57
18	RND	—	7	1	130	2	10.09	10.09	1.26
19	RND	—	1	1	130	2.5	5.18	5.18	2.59

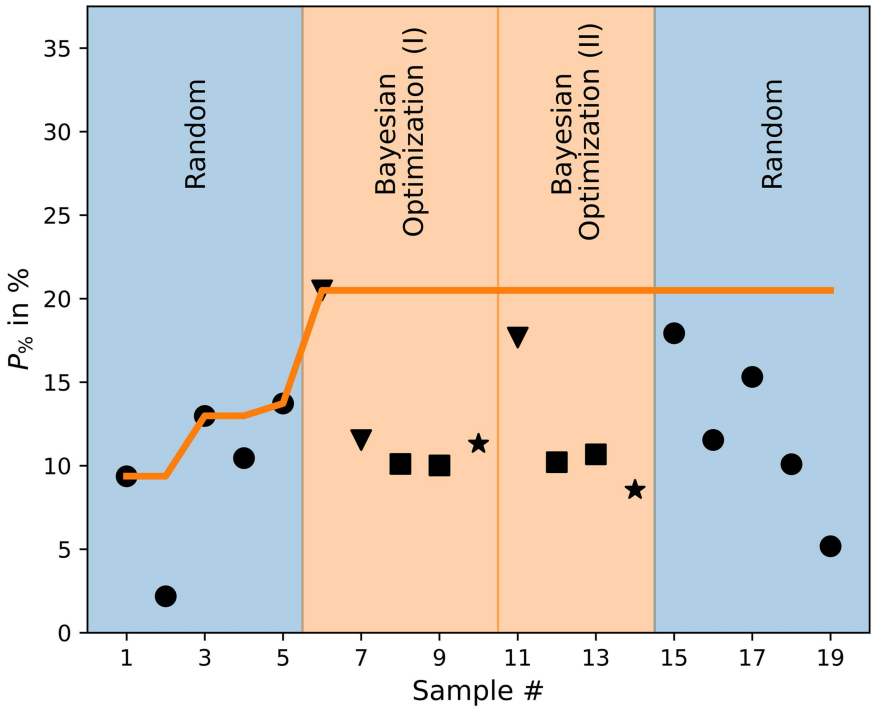

FIGURE 2 | $P_{\%}$ of the SPC and their current maximum (orange line). Random experiments are marked with circles (•), BO of $P_{\%}$ is marked with triangles (▼), BO of η_P is marked with squares (■), and BO of η_{UP} is marked with stars (★).

by other GPR models. Additionally, some proposed formulations do not yield a usable solid product due to an unfavorable urea-to-PA ratio. Heinze and colleagues emphasized the significance of an appropriate urea-to-PA ratio in the phosphatization of starch [1].

The $P_{\%}$ of the initial five random data points ranges from approximately 2.2% to 13.7% (see Table 1). These significant variations in $P_{\%}$ result from differing synthesis conditions. The maximum $P_{\%}$ of 13.7% of the initial five random data points is comparable to values reported in the literature: Heinze and

colleagues reported a maximum $P_{\%}$ of approximately 11.7% [1], while Gebke and colleagues, who used a kneader instead of an oven and monoammonium phosphate as a phosphatizing agent, found a maximum $P_{\%}$ of roughly 12.7% [13].

Using the DP kernel, the BO of $P_{\%}$ proposes the formulation with the highest $P_{\%}$ among all tested experiments, approximately 20.5%. The synthesis conditions corresponding to this result utilize the highest molar ratios of urea and PA within the allowed feature space, indicating that more is better in this context. Specifically, an abundance of PA coupled with an adequate molar ratio of urea is advantageous for achieving high $P_{\%}$. Additionally, elevated synthesis temperatures and extended synthesis durations facilitate the most complete phosphatization possible. In contrast, the RBF kernel operates more locally, proposing a formulation (Experiment 7) that closely resembles the synthesis conditions of the experiment with the maximum $P_{\%}$ of the initial five random data points. This results in a formulation with a slightly lower $P_{\%}$.

The second round of BO of $P_{\%}$ does not result in any improvement, indicating that the optimal synthesis conditions for achieving high $P_{\%}$ have already been determined. Diversifying the data set by adding another five data points leads to the same set of optimal synthesis conditions. Therefore, it is reasonable to conclude that the optimal synthesis conditions among the virtual experiments have already been identified.

There are several reasons why the $P_{\%}$ and the target values derived from it vary with different synthesis conditions. First, phosphorus may be present in various types of functional groups, such as SPC, ammonium starch phosphate, starch carbamate phosphate with blocked amino group, starch phosphoric amide, and starch carbamoyl phosphate [7]. The proportions of hydrogen, carbon, nitrogen, oxygen, and phosphorus in these functional groups vary widely. Notably, regular carbamate groups contain no phosphorus. Therefore, synthesis conditions favoring the formation of functional groups with a high proportion of phosphorus and fewer other elements increase $P_{\%}$.

Second, $P_{\%}$ can be increased by forming ammonium diphosphate, ammonium triphosphate, or ammonium polyphosphate groups, leading to a higher proportion of phosphorus in one AGU. For very high n_{PA}, this is the only mechanism to further increase $P_{\%}$ since the preferred hydroxyl groups of the AGU have already been phosphatized [1].

Third, the pH value determined by n_{urea} and n_{PA} is crucial for successful starch phosphatization [1]. Therefore, a certain ratio between urea and PA is necessary to ensure high $P_{\%}$. However, an over-proportional n_{urea} leads to increased formation of carbamate-type functional groups, reducing $P_{\%}$ due to the higher molecular weight of carbamated AGU [38].

Fourth, high temperatures and long synthesis durations enable the most complete decomposition of urea and potentially even carbamate groups, eliminating non-phosphorous compounds and functional groups from the SPC [10].

Figure 3 displays the η_{P} values of 19 different synthesized SPC formulations, along with the current maximum η_{P} value, indicated by the orange line. The η_{P} of the initial five random data points ranges from approximately 0.5%/mol to 10.5%/mol, suggesting that an overproportional use of PA does not correlate with higher educt efficiency. The first round of BO leads to an improvement in η_{P}, with experiment 10 achieving 11.3%/mol, the maximum value of η_{P} among the tested synthesis conditions.

In general, synthesis conditions resulting in high η_{P} are characterized by using the minimal n_{PA} of one, along with a relatively low n_{urea}. As mentioned previously, high n_{urea} may lead to unnecessary carbamate group formation, which decreases $P_{\%}$ and thereby η_{P}. Similar to the BO of $P_{\%}$, the values for η_{P} plateau, indicating that the maximum η_{P} has likely been reached.

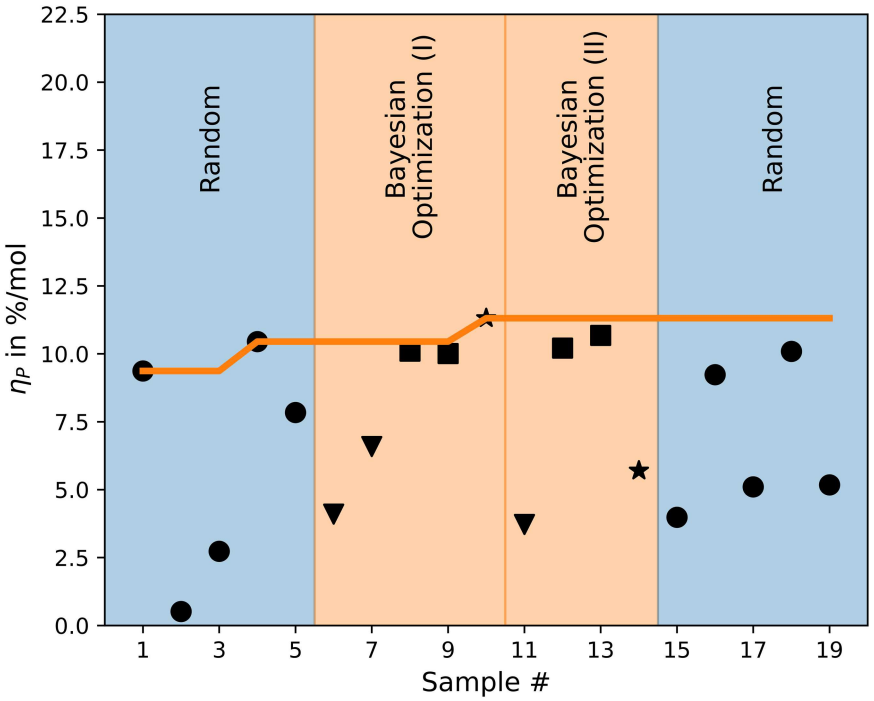

FIGURE 3 | η_{P} of the SPC and their current maximum (orange line). Random experiments are marked with circles (•), BO of $P_{\%}$ is marked with triangles (▼), BO of η_{P} is marked with squares (■), and BO of η_{UP} is marked with stars (★).

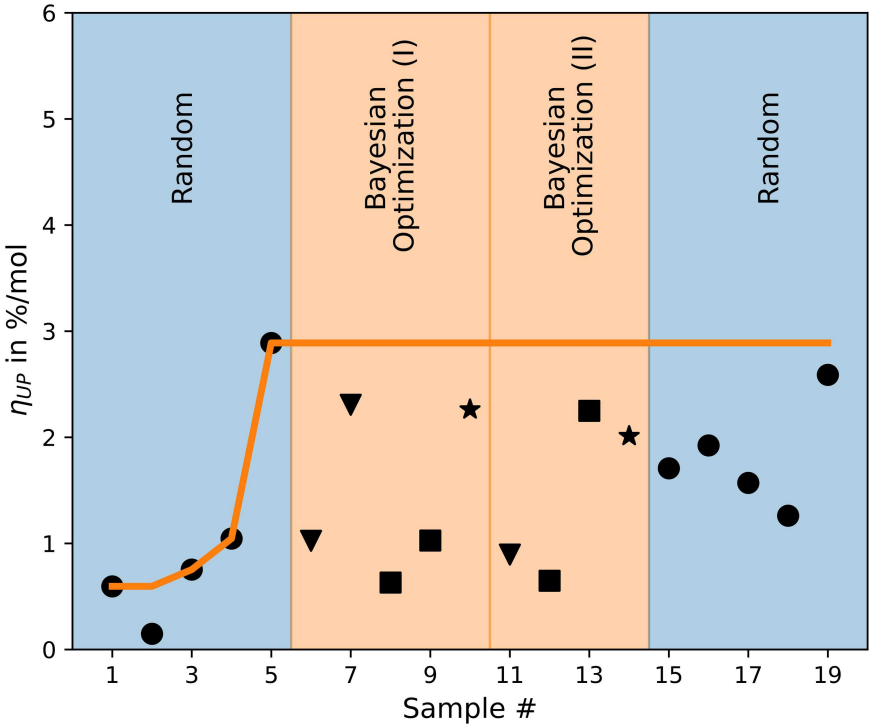

FIGURE 4 | η_{UP} of the SPC and their current maximum (orange line). Random experiments are marked with circles (•), BO of $P_{\%}$ is marked with triangles (▼), BO of η_P is marked with squares (■), and BO of η_{UP} is marked with stars (★).

Figure 4 displays the η_{UP} values of 19 different synthesized SPC formulations, along with the current maximum η_{UP} value, indicated by the orange line. For η_{UP}, BO did not yield improvements over the best results from the initial random experiments. This outcome can be explained by the nature of the η_{UP} metric: it is a ratio of phosphorus content to the combined molar input of urea and phosphoric acid. In this data set, conditions that maximize $P_{\%}$ generally require high reagent loadings, which reduce η_{UP}. Conversely, conditions with high η_{UP} tend to have moderate $P_{\%}$, limiting the maximum attainable value. The highest η_{UP} values occurred in a narrow region of the synthesis space that was already sampled by the initial random experiments. As a result, the BO algorithm, which builds on existing data to explore promising regions, had no opportunity to discover significantly better conditions. This does not indicate a limitation of BO itself, but rather reflects that η_{UP} was already near its global optimum of approximately 2.9%/mol within the explored parameter space after the initial sampling.

4 | Conclusion and Outlook

This study demonstrates how modern machine learning techniques, such as BO, can efficiently tackle complex tasks in chemistry, exemplified by determining the optimal synthesis conditions for specific product properties in SPC phosphatization. By optimizing the molar ratios of the reactants (n_{urea} and n_{PA}), as well as the synthesis temperature and duration, BO effectively enhances the $P_{\%}$ and η_P. The improvements in target properties are achieved in the first BO round with a minimal number of experiments. The maximum values for $P_{\%}$, η_P, and η_{UP} are approximately 20.5%, 11.3%/mol, and 2.9%/mol, respectively. Maximizing these target properties is crucial for the successful synthesis of SPC, ensuring the potency and sustainability of the bio-based FRs.

Acknowledgments

The authors express appreciation to Felix Ludik for his valuable support throughout this research endeavor. Parts of the research documented in this manuscript have been funded by the German Federal Ministry for Economic Affairs and Climate Action (BMWK) within the research project "NewPreg – Nachhaltige, wirtschaftliche und funktionalisierte Bio-Feststoffharz-Prepregtechnologie zur CO2-Reduktion durch kühlfreie Lagerung, Einsatz erneuerbarer Ressourcen und Gewichtsreduktion durch maßgeschneidertes Drapierverhalten" (Grant # 20Q2227C, Germany). Open Access funding enabled and organized by Projekt DEAL.

Conflicts of Interest

The authors declare no conflicts of interest.

Data Availability Statement

The data that support the findings of this study are available from the corresponding author upon reasonable request.

References

1. U. Heinze, D. Klemm, E. Unger, and F. Pieschel, "New Starch Phosphate Carbamides of High Swelling Ability: Synthesis and Characterization," *Starch* 55, no. 2 (2003): 55–60, https://doi.org/10.1002/star.200390017.

2. F. Pieschel, E. Lange, and J. Camacho, "Starch Phosphates, Method for the Production Thereof and Their Use," US Patent 6,703,496 (2004).

3. L. Passauer, F. Liebner, and K. Fischer, " Synthesis and Properties of Novel Hydrogels From Cross-Linked Starch Phosphates," in Macromolecular Symposia, Vol. 244 (Wiley Online Library, 2006), 180–193.

4. L. Passauer, F. Liebner, and K. Fischer, "Starch Phosphate Hydrogels. Part I: Synthesis by Mono-Phosphorylation and Cross-Linking of Starch," *Starch* 61, no. 11 (2009): 621–627.

5. L. Passauer, S. Fischer, H. Bender, S. Tech, and A. Wagenführ, "Use of Water-Soluble Nitrogen- and Phosphorus-Containing Polysaccharide Derivatives as Flame Retardants, Wood Composite Material With Improved Flame Retardance Properties and Process For Its Preparation," Google Patents DE102012204238B4 (2012).

6. L. Passauer, S. Fischer, H. Bender, S. Tech, and A. Wagenführ, "Flame Retardants Comprising Polysaccharide Derivatives Containing Nitrogen and Phosphorus and Use Thereof to Improve the Flame-Retardant Properties of Wood and Wood Composite Materials," Google Patents EP2825615A1 (2013).

7. L. Passauer and H. Bender, "Functional Group Analysis of Starches Reacted With Urea-Phosphoric Acid–Correlation of Wet Chemical Measures With FT Raman Spectroscopy," *Carbohydrate Polymers* 168 (2017): 356–364.

8. L. Passauer, "Thermal Characterization of Ammonium Starch Phosphate Carbamates for Potential Applications as Bio-Based Flame-Retardants," *Carbohydrate Polymers* 211 (2019): 69–74.

9. S. Azeroual, A. Belfkira, H. Wattati, M. Taourirte, and R. Jalal, "Obtaining and Microstructural Study of a Multifunctional Highly Phosphorylated Starch," *Starch* 75, no. 11–12 (2023): 2300071.

10. F. Rothenhäusler, F. Ludik, R. Schneider, et al., "Influence of Post-Synthesis Heat Treatments on the Molecular Structure and Thermal Stability of Phosphatized Starch," *Macromolecular Chemistry and Physics* 226, no. 9 (2025): 2400252, https://doi.org/10.1002/macp.202400252.

11. L. Passauer, "Studies on the Pyrolysis and Potential Flame Retardancy of Low-Substituted Starch Phosphates," *Carbohydrate Polymers* 348 (2025): 122863, https://doi.org/10.1016/j.carbpol.2024.122863.

12. F. Rothenhäusler, F. Ludik, and H. Ruckdaeschel, "Flame Retardant Performance of Phosphatized Starch in Epoxy Resins: A Sustainable Approach to Enhancing Fire Safety," *Journal of Applied Polymer Science* 142, no. 32 (2025): e57273, https://doi.org/10.1002/app.57273.

13. S. Gebke, K. Thümmler, R. Sonnier, S. Tech, A. Wagenführ, and S. Fischer, "Flame Retardancy of Wood Fiber Materials Using Phosphorus-Modified Wheat Starch," *Molecules* 25, no. 2 (2020): 335, https://doi.org/10.3390/molecules25020335.

14. S. Gebke, K. Thümmler, R. Sonnier, S. Tech, A. Wagenführ, and S. Fischer, "Suitability and Modification of Different Renewable Materials as Feedstock for Sustainable Flame Retardants," *Molecules* 25, no. 21 (2020): 5122, https://doi.org/10.3390/molecules25215122.

15. W. Ji, D. Wang, J. Guo, et al., "The Preparation of Starch Derivatives Reacted With Urea-Phosphoric Acid and Effects on Fire Performance of Expandable Polystyrene Foams," *Carbohydrate Polymers* 233 (2020): 115841, https://doi.org/10.1016/j.carbpol.2020.115841.

16. Y. Lu, P. Zhao, Y. Chen, et al., "A Bio-Based Macromolecular Phosphorus-Containing Active Cotton Flame Retardant Synthesized From Starch," *Carbohydrate Polymers* 298 (2022): 120076.

17. F. Schäfer, "Investigations on the Influences of Paper Intrinsic Properties and Flame Retardants on Paper Materials Fire Properties" (PhD thesis, Technische Universität Darmstadt, Darmstadt, 2023).

18. B. Schartel, "Phosphorus-Based Flame Retardancy Mechanisms–Old Hat or a Starting Point for Future Development?," *Materials* 3, no. 10 (2010): 4710–4745.

19. S. Huo, P. Song, B. Yu, et al., "Phosphorus-Containing Flame Retardant Epoxy Thermosets: Recent Advances and Future Perspectives," *Progress in Polymer Science* 114 (2021): 101366, https://doi.org/10.1016/j.progpolymsci.2021.101366.

20. L. Passauer, " P–N-Modified Starch: A Polymeric Flame Retardant for Wood-Based Materials," in Bio-Based Flame-Retardant Technology for Polymeric Materials, ed. Y. Hu, H. Nabipour, and X. Wang (Elsevier, 2022), 339–368.

21. C. J. Taylor, K. C. Felton, D. Wigh, et al., "Accelerated Chemical Reaction Optimization Using Multi-Task Learning," *ACS Central Science* 9, no. 5 (2023): 957–968.

22. G. Luo, X. Yang, W. Su, T. Qi, Q. Xu, and A. Su, "Optimizing Telescoped Heterogeneous Catalysis With Noise-Resilient Multi-Objective Bayesian Optimization," *Chemical Engineering Science* 298 (2024): 120434.

23. N. P. Romer, D. S. Min, J. Y. Wang, et al., "Data Science Guided Multiobjective Optimization of a Stereoconvergent Nickel-Catalyzed Reduction of Enol Tosylates to Access Trisubstituted Alkenes," *ACS Catalysis* 14, no. 7 (2024): 4699–4708.

24. M. M. Velencoso, A. Battig, J. C. Markwart, B. Schartel, and F. R. Wurm, "Molecular Firefighting–How Modern Phosphorus Chemistry Can Help Solve the Challenge of Flame Retardancy," *Angewandte Chemie International Edition* 57, no. 33 (2018): 10450–10467, https://doi.org/10.1002/anie.201711735.

25. S. Rabe, Y. Chuenban, and B. Schartel, "Exploring the Modes of Action of Phosphorus-Based Flame Retardants in Polymeric Systems," *Materials* 10, no. 5 (2017): 455.

26. J. Green, "A Review of Phosphorus-Containing Flame Retardants," *Journal of Fire Sciences* 10, no. 6 (1992): 470–487, https://doi.org/10.1177/073490419201000602.

27. J. Hastie, "Molecular Basis of Flame Inhibition," *Journal of Research of the National Bureau of Standards. Section A, Physics and Chemistry* 77, no. 6 (1973): 733.

28. B. J. Shields, J. Stevens, J. Li, et al., "Bayesian Reaction Optimization as a Tool for Chemical Synthesis," *Nature* 590, no. 7844 (2021): 89–96.

29. E. Braconi and E. Godineau, "Bayesian Optimization as a Sustainable Strategy for Early-Stage Process Development? A Case Study of Cu-Catalyzed C–N Coupling of Sterically Hindered Pyrazines," *ACS Sustainable Chemistry & Engineering* 11, no. 28 (2023): 10545–10554.

30. Y. Wu, A. Walsh, and A. M. Ganose, "Race to the Bottom: Bayesian Optimisation for Chemical Problems," *Digital Discovery* 3, no. 6 (2024): 1086–1100.

31. C. E. Rasmussen and C. K. I. Williams, *Gaussian Processes for Machine Learning* (MIT Press, 2006).

32. T. Danka and P. Horvath, "A Modular Active Learning Framework for Python," preprint, arXiv, https://arxiv.org/abs/1805.00979.

33. F. Rothenhäusler and H. Ruckdaeschel, "Strategies for the Fast Optimization of the Glass Transition Temperature of Sustainable Epoxy Resin Systems via Machine Learning," *Journal of Applied Polymer Science* 141, no. 21 (2024): e55422, https://doi.org/10.1002/app.55422.

34. E. Brochu, V. M. Cora, and N. De Freitas, "A Tutorial on Bayesian Optimization of Expensive Cost Functions, With Application to Active User Modeling and Hierarchical Reinforcement Learning," preprint, arXiv: 1012.2599 (2010).

35. D. Duvenaud, "Automatic Model Construction With Gaussian Processes" (PhD thesis, 2014).

36. J. Snoek, H. Larochelle, and R. P. Adams, "Practical Bayesian Optimization of Machine Learning Algorithms," in *Advances in Neural Information Processing Systems*, Vol. 25 (2012).

37. N. Srinivas, A. Krause, S. M. Kakade, and M. Seeger, "Gaussian Process Optimization in the Bandit Setting: No Regret and Experimental Design," preprint, arXiv: 0912.3995 (2009).

38. M. Khalil, S. Farag, K. M. Mostafa, and A. Hebeish, "Some Studies on Starch Carbamate," *Starch* 46, no. 8 (1994): 312–316.